의학석사 학위논문

STIM1 and SERCA Regulate Spike Frequency Adaptation and Intrinsic Excitability of Mouse Cerebellar Purkinje Neurons

STIM1과 소포체칼슘펌프에 의한 생쥐 소뇌 퍼킨지 신경세포의 신호 자가 억제와 내인 흥분성의 조절

2018년 2월

서울대학교 대학원
의과학과 생리/신경과학전공
정 다 윤

STIM1과 소포체칼슘펌프에 의한 생쥐 소뇌 퍼킨지 신경세포의 신호 자가 억제와 내인 흥분성의 조절

지도교수 김 상 정

이 논문을 의학석사 학위논문으로 제출함
2017년 10월

서울대학교 대학원
의과학과 생리/신경과학전공
정 다 윤

정 다 윤의 의학석사 학위논문을 인준함
2017년 1월

위 원 장 (인)
부위원장 (인)
위 원 (인)

STIM1 and SERCA Regulate Spike Frequency Adaptation and Intrinsic Excitability of Mouse Cerebellar Purkinje Neurons

By

Dayoon Jung

A Thesis Submitted to the Department of Biomedical Sciences in Partial Fulfilment of the Requirements for the Degree of Master of Science in Medicine (Physiology/Neuroscience) at Seoul National University College of Medicine

January 2018

Approved by thesis committee:

Professor _____ (Chairman)

Professor _____ (Vice chairman)

Professor _____

Abstract

STIM1 and SERCA regulate spike frequency adaptation and intrinsic excitability of mouse cerebellar Purkinje neurons

Dayoon Jung
Department of Biomedical Sciences
Graduate School
Seoul National University

Proper regulation of cytosolic calcium is important for various neuronal functions. Endoplasmic reticulum (ER) is the main internal calcium store where cytosolic calcium comes in and out appropriately depending on the situations. Recent studies have discovered that stromal interaction molecule 1 (STIM1), which regulates ER store calcium, is widely expressed in the brain, especially in the cerebellar Purkinje neurons. Previous study showed that STIM1 mediates mGluR1-dependent slow current in Purkinje neurons. However, this experiment could not suggest any convincing role of STIM1 in spontaneously firing neurons. Here, by using Purkinje neuron-specific STIM1 knock out mice ($STIM1^{PKO}$), I investigated the functional role of STIM1 in Purkinje neuron. It was found that the loss of STIM1 resulted in reduced intrinsic excitability with increased spike frequency adaptation (SFA), which was attributed to altered Ca^{2+}-dependent K+ (Kca) current. Furthermore, blocking Sarco/endoplasmic reticulum Ca2+ ATPase (SERCA) altered intrinsic properties of $STIM1^{WT}$ to the same level of $STIM1^{PKO}$ while $STIM1^{PKO}$ was unaffected. These findings suggest that STIM1 plays an important role in regulating proper neuronal firing of Purkinje

neuron by handling cytosol calcium with SERCA.

Keywords: Purkinje neuron, spontaneous firing neuron, intrinsic excitability, STIM1, ER Ca^{2+} store, SERCA

Student Number: 2013 – 21789

Contents

List of Figures and Tables

Introduction

Cytosolic calcium plays important roles in various cellular function such as transcription, cell growth and apoptosis and especially in neurons, they can affect many neuronal functions including neuronal plasticity, excitability and synaptic transmission (Mattson et al., 2000; Erwin and Sakaba, 2008). The concentration of cytosolic calcium is regulated dynamically by the calcium fluxes from both extracellular space and internal store.

Endoplasmic reticulum (ER) is the main internal calcium store which can causes both cytosolic calcium influx and efflux. ER releases calcium via inositol 1, 4, 5-triphosphate receptors (IP3Rs) and ryanodine receptors (RyRs) (Verkhratsky, 2005). These forms of calcium flux can be sustainable when ER store retains sufficient calcium to release. A stromal interaction molecule (STIM) protein, localized to ER membrane, is well known for its crucial role in refilling ER calcium when store is depleted (Soboloff et al., 2012). STIM protein has a EF-hand motif, a kind of calcium sensor, in the ER lumen so that they can be activated when ER calcium is low. As STIM protein is activated, it clusters and gates store-operated channels (SOCs) on plasma membrane. Extracellular calcium enters through SOCs, which is referred to as store-operated calcium entry (SOCE), and sarco/endoplasmic reticulum calcium ATPase (SERCA) pumps calcium into ER which would be cytosolic calcium efflux. STIM protein is widely expressed in many cell types including immune, muscle and neuronal cells. Many researchers have figured out the role of STIM in immune and muscle cells (Zhang et al., 2005; Ritchie et al., 2012; Stiber, et al., 2008) but the neuronal functions of STIM have just begun to be identified (Hartmann et al., 2014; Sun et al., 2014).

Purkinje neuron is the central neuron of cerebellar cortex, integrating sensory-

motor inputs via parallel fiber and mossy fiber and providing the sole output of cerebellar cortex (Dean et al., 2010). Purkinje neuron has distinct feature that it spontaneously generates action potentials with high-frequency in the absence of synaptic input. This feature is highly important for conducting accurate cerebellar functions as many studies showed that interference in spontaneous firing pattern induced severe deficits in cerebellar behavior (Hoebeek et al., 2005; Wulff et al., 2009). Normal spike firing can be maintained through the harmony of sodium, potassium and calcium ion channels (Bean, 2007). Especially, in this high-frequency spiking neurons different from other cell types, huge amounts of calcium entry occur through continuously opened voltage-gated calcium channels (VGCCs) and they need to be handled consequently.

Among all brain regions, cerebellar Purkinje neurons have highest expression of type 1 STIM (STIM1) proteins (Skibinska-Kijek et al., 2009). So far, most studies have focused on the canonical role of STIM1 for ER stress (low $[Ca^{2+}]_{ER}$). However, Purkinje neurons have spontaneous firing activity and abundant cytosolic calcium environment accordingly. It means ER stores in Purkinje neurons are regarded to have less chance to be depleted than those in the other neurons. In this point of view, further explanation functional role of STIM1 in Purkinje neuron is demanded.

Despite of the high expression level of STIM1 in Purkinje neuron, only one study has reported the role of STIM1 in Purkinje neuron. Hartmann et al. suggested that STIM1 mediates metabotropic glutamate receptor type 1 (mGluR1) and transient receptor potential channel 3 (TRPC3) current (Hartmann et al., 2014). They showed both mGluR1-dependent current and ER store calcium are strongly attenuated in the absence of STIM1. However, these experiments were performed in -70mV voltage-clamp (VC) mode and in dendritic region. Although Hartmann et al. showed in one experiment that

both dendritic mGluR1-dependent slow current and ER store calcium can be transiently restored after somatic depolarization, they did not provide satisfactory explanation. It should be considered that Purkinje neurons are continually depolarized in physiological conditions and also, ER compartment is extended to distal dendritic branch with continuity (Terasaki et al., 1994).

In this study, we investigated the functional role of STIM1 in Purkinje neuron. By using Purkinje neuron-specific STIM1 knock-out ($STIM1^{PKO}$) mice, we found that STIM1 contributes to SERCA-dependent cytosolic calcium clearance in firing Purkinje neuron, which affects calcium-activated potassium (Kca) channel and changes intrinsic firing properties; decreased firing frequency with increased spike frequency adaptation. These results highlight the importance of ER store and the novel role of STIM1 in firing neuron.

Materials and Methods

Animals

STIM1^{PKO} mice were generated by crossing the homozygous PCP2-Cre line (B6.129-Tg(Pcp2-cre)2Mpin/J line from The Jackson Laboratory) with the STIM1-floxed line (C57BL/6 background). The first filial generation (F1) was crossed again with the STIM1-floxed line. Among the second filial generation (F2), male mice that were homozygous for floxed-STIM1 alleles were used for this study. We used male mice in all of the experiments. All procedures were approved by the Institutional Animal Care and Use Committee of Seoul National University College of Medicine.

PCR

Generated STIM1^{PKO} mice were genetically confirmed by existence or nonexistence of Stim1 gene. DNAs were extracted from cerebellar brain tissue with 20μl 25mM NaOH + 0.25mM EDTA solution at 98℃ for 30min and 20μl Tris-HCl (pH5.5) was added. Used primer pairs were; Forward = 5'-GCTAGCAGTAACCAACACCACCATG-3', Reverse = 5'-GATCTCATCTCGCAGCTTCTTCTCC-3'. Target gene included exon 5, exon 6 and partial exon 7 so that deletion of exon 6 could be recognized by its product size; STIM1^{WT} (exon 5 + exon 6 + partial exon 7) = 373bp, STIM1^{PKO} (exon 5 + partial exon7) = 195bp.

Immunohistochemistry

Anesthetized 9- and 13-week-old mice were perfused with phosphate buffered saline (PBS, Gibco, Life Technologies, UK) and 4% paraformaldehyde (PFA, Tech&Innovation, Korea) in turn. Brains were taken out and fixed in 4% PFA overnight.

After having the tissues embedded in paraffin, we obtained 5-μm thick sagittal slices on slides by using a microtome (Leica, Germany). Paraffin was removed with 3 changes of 100% xylene (Junsei Chemical, Japan) and the xylene was washed out with 3 changes of 99.9%, 2 changes of diluted 95%, 90%, 80% and 70% ethanol (Sigma-Aldrich, UK). Then, slides were submerged in distilled water for their hydration. Epitope retrieval was performed with heated citrate buffer (pH 6.0, Tech&Innovation, Korea). After PBS washing, slices were blocked with the serum solution containing PBS-T (0.3% Triton X-100) and 5% goat serum (Vector Laboratories, Burlingame, USA) for 1 hour at room temperature. The slices were, then, incubated with diluted primary antibodies, anti-STIM1 (rabbit, 1:500, Cell Signaling, USA) and Calbindin (mouse, 1:500, Abcam, USA), overnight at 4˚C. After washing in PBS, fluorescence-conjugated secondary antibodies, Alexa-488 and 568 (anti-rabbit; 1:500, anti-mouse; 1:500, Abcam, USA), were treated to the slices for 1 hour at room temperature. Primary antibodies and secondary antibodies were diluted in serum solution and PBS, respectively. Images were acquired and processed using a confocal microscope (confocal A1, Nikon, Japan) and NIS-Element software (Nikon, Japan).

Electrophysiology

Slice preparation.

Sagittal slices of the cerebellar vermis (250μm thick) were obtained from 6- to 9-week-old mice using a vibratome (Leica VT1200, Germany) after isoflurane anesthesia and decapitation. The slices were cut with ice-cold cutting solution containing (in mM): 75 sucrose, 75 NaCl, 2.5 KCl, 7 $MgCl_2$*$6H_2O$, 0.5 $CaCl_2$*$6H_2O$, 1.25 NaH_2PO_4, 26 $NaHCO_3$, 25 glucose, bubbled with 95% O_2 and 5% CO_2. After cutting, the slices were

immediately moved into the warmed (32˚C) chamber with artificial CSF (ACSF) containing (in mM): 125 NaCl, 2.5 KCl, 1 $MgCl_2$*$6H_2O$, 2 $CaCl_2$*$2H_2O$, 1.25 NaH_2PO_4, 26 $NaHCO_3$, 10 glucose bubbled with 95% O_2 and 5% CO_2. For recovery, slices were kept for 30min at 32˚C and 1hr at RT. All recordings were done within 8hrs from recovery.

Whole-cell and Cell-attached recordings.

Brain slices were placed in a submerged chamber and perfused with ACSF for at least 10 min before recording. Somatic whole-cell VC and current-clamp (CC) recordings were made at 29.5-30°C. We used recording pipettes (3– 4 M) filled with the following (in mM): 9 KCl, 10 KOH, 120 K-gluconate, 3.48 $MgCl_2$, 10 HEPES, 4 NaCl, 4 Na_2ATP, 0.4 Na_3GTP, and 17.5 sucrose, pH 7.25. For cell-attached recordings, experiments were performed at 32–32.5°C by using recording pipettes (4–5 M) filled with the following (in mM): 125 NaCl, 10 HEPES, 3 KCl, and 2 $CaCl_2$. Low Ca^{2+}-ACSF contained a lower Ca^{2+} concentration (100μM), and a reduced amount of $CaCl_2$ was substituted with an equivalent amount of $MgCl_2$. Data were acquired using an EPC9 patch-clamp amplifier (HEKA Elektronik) and PatchMaster software (HEKA Elektronik) with a sampling frequency of 20 kHz, and the signals were filtered at 2 kHz. All electrophysiological recordings were acquired in Lobule III–V of cerebellar central vermis, except for the data presented in Figure 3B (right).

Stimulations.

To induce mGluR1-dependent slow current, parallel fibers (PFs) were stimulated (10 pulses, 100Hz) by ACSF-containing glass pipettes onto the molecular layer (ML) under

100μM picrotoxin and 2.5μM NBQX. 2.5μM NBQX was for blocking ~90% AMPA receptors to avoid excessive current.

Drugs.

In the experiments for measuring intrinsic excitability, all of the recordings were performed within the ACSF containing 10μM 2,3-dihydroxy-6-nitro-7-sulfamoyl-benzo[f]quinoxaline (NBQX) and 100μM picrotoxin to block excitatory and inhibitory synaptic inputs, respectively. All drugs used in the experiments, except for picrotoxin (Sigma-Aldrich), were purchased from Tocris Bioscience.

Data analysis.

All patch-clamp data was imported and analyzed using Igor Pro (WaveMetrics) and NeuroMatic (ThinkRandom) plug-in. Pooled data underwent further analysis using software custom built with LabView (National Instruments). Membrane capacitance (Cm) was measured from a current trace of a 5 mV depolarizing voltage-step (50ms duration), and input resistance (Rin) was measured from the end of the voltage trace of 100pA hyperpolarizing current step (1s duration). Active membrane properties were analyzed from the action potential train induced by a 600pA depolarizing current injection (1s duration). The threshold was determined by measuring the membrane potential where its velocity entered the range of 30–60 mV/ms (Kim et al., 2012). AP amplitude was calculated as a difference between the threshold and positive peak. Upstroke and downstroke were measured as the maximal derivative of the voltage with respect to time (dV/dt) ratio of the rising and falling phases, respectively. The slope of postspike depolarization was measured as the slope between the negative peak of the

target spike and the threshold of the next spike that covers the interaction potential window, while the inter-spike interval (ISI) was assessed as the time difference between positive peaks of the target spike and the next spike that covers both action potentials and interaction potential windows. Fast afterhyperpolarization (fAHP) and medium AHP (mAHP) were measured by subtracting the negative peak of the end of the action potential and the action potential train from both the threshold and -70 mV baseline.

Western blot

Tissues were lysed with 1% Triton X-100, 300mM NaCl, 50mM Tris-HCl, 500mM NaF, 200mM Na_3VO_4, protease inhibitor cocktail (P8340, Sigma-Aldrich) and phosphatase inhibitors (Cocktail2; P5726, Cocktail3; P0044, Sigma-Aldrich, UK). Quantitative analysis was performed by BCA assay (Pierce BCA kit, Life Technologies, UK) and the equal amount of proteins were loaded onto SDS-PAGE on 8%-13% acrylamide gels. After blocking by 5% skim milk in TBS-T (TBS with 0.1% tween-20), blots were incubated overnight with primary antibodies at 4°C. Primary antibodies were: monoclonal mouse anti-calbindin (1:1000, CB955, Abcam, USA), polyclonal goat anti-parvalbumin (1:1000, Swant, Switzerland) and monoclonal mouse anti-α tubulin (1:10000, TU-02, Santa Cruz Biotechnology, USA). After washing with PBS-T, blots were then incubated for 1 hour with secondary antibodies. Secondary antibodies were: HRP-conjugated goat anti-mouse IgG (1:1000-10000, BioRad, Germany) and HRP-conjugated rabbit anti-goat IgG (1:2000, BioRad, Germany). After being developed using ECl solution (Super Signal West Pico Chemiluminescent Substrate, Life Technologies, UK), blots were then exposed in Amersham Imager 600 (Amersham/GE Healthcare, Pittsburg) and stored in JPG and TIFF file format. Protein quantification was

performed using ImageJ software (NIH) and each band density was normalized to α tubulin in same lane.

Statistics

Extracted data were managed with Origin 8.5 (OriginLab), with which simple statistics carried out. Further statistical analysis was performed using SPSS Statistics 21 (IBM) or custom built LabView (National Instruments). Student's *t* test and ANOVA as parametric analysis were used each for 2- and more than 3-group-comparison, and in nonparametric case, Mann-Whitney U test and Kruskal-Wallis test was used to each comparison.

Results

The generation of Purkinje neuron-specific STIM1 knock-out ($STIM1^{PKO}$) mice

To investigate the role of STIM1 in Purkinje neuron, we generated Purkinje neuron-specific STIM1 knock-out ($STIM1^{PKO}$) mice by selectively removing exon 6 (which is translated into the transmembrane domain of STIM1) of the *stim1* gene under Cre/loxP system (Figure 1A). PCR and immunostaining data showed that Cre/loxP system successfully worked in that the samples identified by PCR experiment were double-confirmed by immunostaining with STIM1 antibody (Figure 1B, C).

Depolarization recovers lowered mGluR1-dependent slow current in $STIM1^{PKO}$

A previous study demonstrated that Purkinje neurons lack of STIM1 have strongly attenuated metabotropic glutamate receptor type 1 (mGluR1)-dependent slow current and IP3 receptor-dependent Ca^{2+} signals (Hartmann et al., 2014). Also, they showed that these attenuations were transiently restored after 1sec-somatic depolarization. As we used different promotor (Pcp2, Hartmann; GluD2) for generation of $STIM1^{PKO}$ mice, we confirmed whether identical phenomena reproduced in our conditions. Furthermore, to describe the phenomena in detail, we tested 200msec, 500msec and 1sec depolarization. As a result, STIM1 lacking Purkinje neuron showed lowered mGluR1-dependent slow current at resting potential (-70mV) but recovered after 200ms-, 500ms or 1sec-somatic depolarization (0mV) (200ms; Figure 2, 500ms, 1sec; data not shown). Rescued mGluR1-dependent slow current, which is proportional to ER Ca^{2+} store (Hartmann et al., 2014), prolonged up to few minutes where no more depolarization was occur (Figure 2A, B). Repetitive depolarization for every one minute was enough to sustain mGluR1-

dependent slow current and ER Ca^{2+} store continuously (Figure 2B, orange). There was no significant change in AMPA-dependent current (fast current, Figure 2C).

Decreased intrinsic excitability with altered firing pattern in STIM1^{PKO}

Considering that Purkinje neurons are pacemaker cell, we measured spontaneous firing activity without glutamatergic and GABAergic synaptic inputs in cell-attached mode. Consequently, Purkinje neuron in STIM1^{PKO} showed lowered spontaneous firing rates in both anterior and posterior lobules which are known to have different characteristics along Zebrin-pattern (Zhou et al., 2014) (Figure 3A, B) and higher coefficient of variation (CV) which represents irregularity of spiking (Figure 3C, D). To investigate the details of spike properties, we injected step current into Purkinje neuron in current-clamp mode. The firing frequency versus injected current (*f*-I) curve showed the reduced intrinsic excitability of Purkinje neurons in STIM1^{PKO} mice (Figure 4A-C) with considerably increased mAHP (Figure 4D, E, Table 1).

As lowered excitability and increased mAHP were often observed with increased spike frequency adaptation (SFA) (Benda and Herz, 2003; Belmeguenai et al., 2010), we analyzed instantaneous firing rates (1/inter-spike interval (ISI)) of proceeding spike train. In comparison with same current-injected trains, STIM1^{PKO} exhibited increased SFA compared to STIM1^{WT} (Figure 5A, B). We also noticed that early instantaneous frequencies were not different while late instantaneous frequencies were significantly lowered in almost all step current- injected trains in STIM1^{PKO} (Figure 5C). These results suggest that lowered firing frequency was due to its increased SFA.

However, there was another change in intrinsic properties; input resistance (Rin, Table 1). To exclude the possibility that lowered frequency by changes in input

resistance might provide increased SFA secondarily, we compared SFA among same frequency-bin trains. As a result, SFA was equally observed in that ratio of 1st to 20th ISI was significantly increased in STIM1^{PKO} (Figure 5D, E). This demonstrates that the decrease in intrinsic excitability and the increase in SFA are remarkable changes in STIM1^{PKO}.

Altered Ca2+ concentration makes difference between STIM1^{WT} and STIM1^{PKO}

To determine how STIM1 on ER membrane could affect intrinsic excitability of Purkinje neurons, we fist examined the effect of Ca^{2+} which would be primarily altered under STIM1 lacking environment. We replaced most of the extracellular Ca^{2+} with equivalent amount of Mg^{2+} to exclude Ca^{2+} effect on firing and measured spontaneous firing rates over time. Lowered Ca^{2+} caused the large gap of the firing rates between STIM1^{WT} and STIM1^{PKO} became small and narrowed the gap between the two groups could be recovered after reperfusion of normal ACSF (Figure 6A, B). This result confirmed that the difference in simple spike firing was attributed to altered Ca^{2+} concentration.

The effect of SOCE on spontaneous firing of Purkinje neurons

Due to the role of STIM1 in generating SOCE, we investigated the impact of SOCE to the spontaneous firing of Purkinje neurons. As there was few or no specific blocker for SOCE, we used non-specific blockers: SKF 96365 (30μM), 2-APB (50μM), TRIM (400μM), FFA (100μM). However, they all changed firing pattern of Purkinje neuron and finally caused firing failure so we could not exactly measure or compare effects of SOCE on firing (Figure 7A). Next, we examined the effect of the direct binding of

STIM1 to molecules on plasma membrane. As application of ML-9 (50μM), STIM1-plasma membrane interaction blocker, reduced firing rate without changing the pattern but made the failure of firing (Figure 7A), we used low-dose of ML-9 (10μM). However, it could not narrow the difference of firing rate between two groups (Figure 7B).

Kca current is increased in STIM1^{PKO}

Altered Ca2+ dynamics could affect diverse kinds of Ca^{2+}-dependent ionic channels on plasma membrane. Ca^{2+}-activated K^{+} (Kca) current is well established component through many studies by its effect on excitability of Purkinje neurons (Edgerton and Reinhart, 2003; Benton et al., 2013). Furthermore, it has been known to have strong relation to mAHP and SFA (Benda and Herz, 2003; Belmeguenai et al., 2010) which are also primary changes in STIM1^{PKO} as mentioned above (Figure 3-5). Therefore, it is plausible that altered Ca^{2+} dynamics in STIM1^{PKO} caused changes in Kca current, which lowered intrinsic excitability with mAHP and SFA increased. To verify this hypothesis, we tested the effect of Kca current on spontaneous firing by modulating Kca current. Kca channels are classified into mainly two channels; small conductance Kca (SK) channel and large conductance Kca (BK) channel and they can be selectively blocked by apamin and iberiotoxin (or paxilline), respectively. To find out which current most contributed to the gap between STIM1^{WT} and STIM1^{PKO}, we applied apamin, iberiotoxin and paxilline each during recording spontaneous firing (Figure 8A). As a result, blocking only single SK or BK current couldn't narrow the gap in firing rates of STIM1^{WT} and STIM1^{PKO}. Instead, blocking both SK and BK current by using cocktail of apamin and paxilline could make firing rates of STIM1^{PKO} equal to that of STIM1$^{WT.}$ (Figure 8B).

However, in both groups, the application of an apamin and paxilline cocktail induced burst firing of Purkinje neurons, which is involved in dendritic Ca^{2+} signals (Brenowitz et al., 2006), so we could not precisely estimate the contribution of K_{Ca} channels to simple spike firing and somatic Ca^{2+} signals. Owing to excessive effect of blocking both SK and BK channels, we enhanced them alternatively by using 1-EBIO, a nonselective activator of K_{Ca} channels (Benton et al., 2013) (Figure 8C). Finally, activation both SK and BK channels lowered spontaneous firing rates of both groups to the same level without changing the firing pattern. The effect of 1-EBIO was larger in $STIM1^{WT}$ than $STIM1^{PKO}$ and this result can be considered as Kca current is enhanced in $STIM1^{PKO}$.

The effect of CICR on spontaneous firing of Purkinje neurons

There are several reports showing Ca^{2+}-induced Ca^{2+} release (CICR) whereby stored Ca2+ release through ryanodine receptor (RyR) or Ca^{2+} release through IP3R are coupled with Kca channels (Yamada et al., 2004; Akita and Kuba, 2000). As there existed the possibility that deletion of STIM1 could alter Ca2+ dynamics in ER store, by using dantrolene or low dose of 2-APB (Ju et al., 2011), we examined the effect of Ca^{2+} release through RyR or IP3R on spontaneous firing rate and found that they had no significant effect on spontaneous firing (Figure 7C, D).

STIM1-assisted SERCA is the modulator of Kca current

STIM1s have been well known for its crucial role in refilling ER calcium when store is depleted. They not only bring extracellular Ca^{2+} into cytosol by interacting with SOCs on plasma membrane, but also assist SERCAs that pump entered cytosolic Ca^{2+} into ER

lumen (Soboloff et al., 2012). Above data displaying decreased intrinsic excitability due to enhanced Kca channels imply that cytosolic Ca^{2+} might be increased in $STIM1^{PKO}$. Moreover, in Figure 5 (analysis on SFA), we found that 'the more action potentials proceed over time, the bigger differences in firing rate are made between two groups'. With these results, we assumed that entered Ca^{2+} by action potential was not cleaned properly because of hypofunction of SERCA in $STIM1^{PKO}$ so that there appeared cytosolic Ca^{2+} accumulation by repetitive action potentials. To verify this assumption, we examined the effect of cyclopiazonic acid (CPA, a SERCA inhibitor) on intrinsic properties of two groups. As a result, CPA reduced spontaneous firing rates of $STIM1^{WT}$ while it did not change the rates of $STIM1^{PKO}$ (Figure 9A). Furthermore, CPA made current-evoked firing rate, mAHP and SFA (mainly altered intrinsic factor in $STIM1^{PKO}$) of $STIM1^{WT}$ to the same level of $STIM1^{PKO}$ and, in the same manner, those of $STIM1^{PKO}$ were not affected by CPA (Figure 9B-D). These results suggest that reduced intrinsic excitability of $STIM1^{PKO}$ was induced by declined function of STIM1-assisted SERCA, leading to accumulation of cytosolic Ca^{2+} and its influence on Kca current.

The expression of Ca^{2+} buffer protein is not altered in $STIM1^{PKO}$

Ca^{2+}-binding proteins are generally divided into two groups: Trigger-type and Buffer-type. In Purkinje neurons, large portions of buffer-type Ca^{2+}-binding proteins are comprised of Calbindin-D28k and parvalbumin (Bastianelli, 2003). By western blotting, we could exclude the possibility of Ca^{2+}-binding protein-derived change in Ca^{2+} buffer capacity (Figure 10).

Figure 1

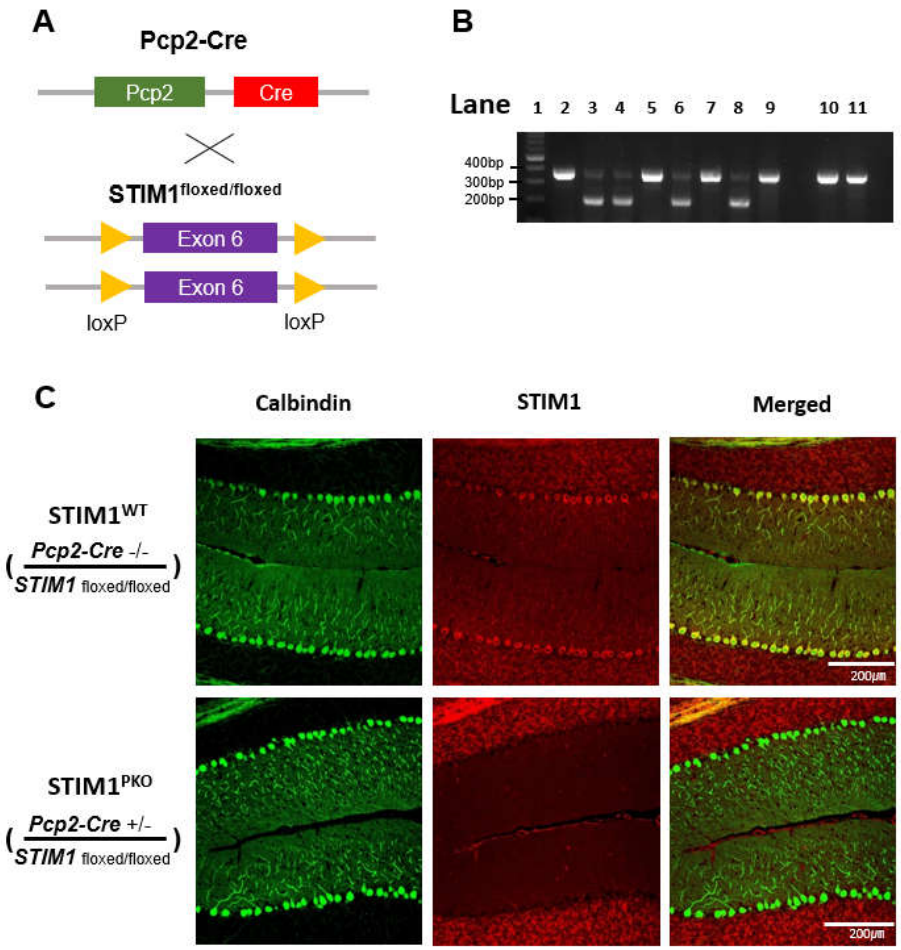

Figure 1. The Generation of Purkinje neuron-specific STIM1 knock-out (STIM1^{PKO}) mice.

A, Schematic strategy for generating STIM1^{PKO} mice. **B**, PCR data showed that the length of target gene of STIM1^{PKO} (lane 3, 4, 6, 8) was shorter than that of STIM1^{WT} (lane 2, 5, 7, 9) or C57BL/6 (lane10, 11). DNA ladder (lane 1). Details in Materials and Methods. **C**, STIM1 was completely abolished in STIM1^{PKO}. Calbindin (green), STIM1 (red), merged from left to right.

Figure 2

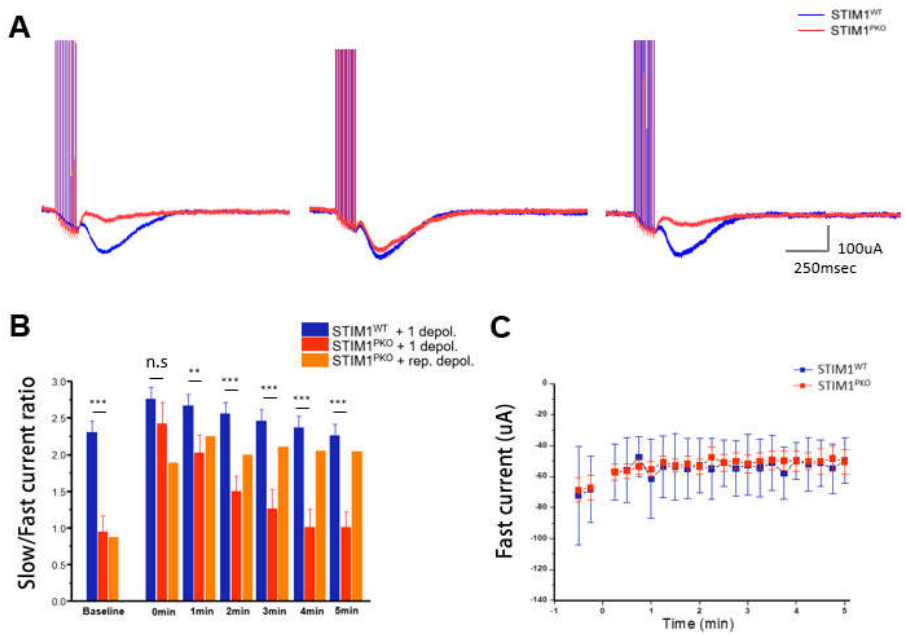

Figure 2. mGluR1-dependent slow current of STIM1^{PKO} was recovered after depolarization. **A**, Representative traces of mGluR1-dependent slow current. Merely little slow current was observed in STIM1^{PKO} (left), but 200ms of brief depolarization fully compensated the slow current to level of STIM1^{WT} (middle). The slow current became little as baseline in 3min after depolarization (right). **B**, Bar graph showing time dependent decaying of recovered slow current in STIM1^{PKO}. Repetitive 200ms of brief depolarization (every 1 min) sustained the slow current to the level of STIM1^{WT} continuously. **C**, No significant change in AMPA-dependent fast current. Asterisks in bar graph were marked by Mann-Whitney U test. Error bars denote SEM. **p<0.01, ***p<0.001.

Figure 3

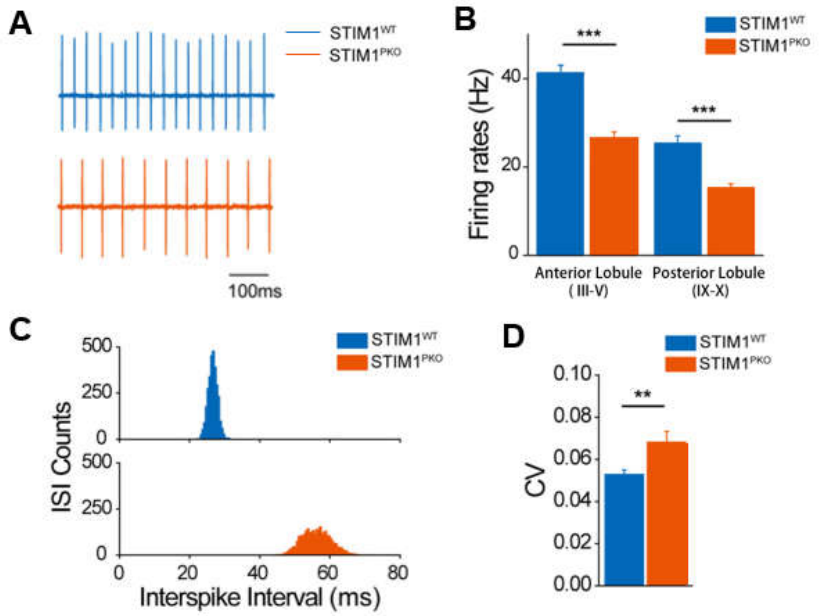

Figure 3. Spontaneous firing rate was reduced both in anterior and posterior region with altered firing pattern in STIM1^{PKO}.

A, Representative traces of spontaneous firing from attached recording in the anterior lobule (III–V) of STIM1^{WT} (blue) and STIM1^{PKO} (red). **B**, Spontaneous simple spike firing frequency was considerably reduced in STIM1^{PKO}. Reduced firing frequency of STIM1^{PKO} was not only observed in anterior lobule (III–V, STIM1^{WT}, n = 13; STIM1^{PKO}, n = 12), but also posterior lobule (IX-X, STIM1^{WT}, n = 14; STIM1 PKO, n = 26). **C**, Distribution plot of corresponding inter-spike interval. **D**, CV was significantly increased in STIM1^{PKO} (STIM1^{WT}, n = 31; STIM1^{PKO}, n = 26).

Figure 4

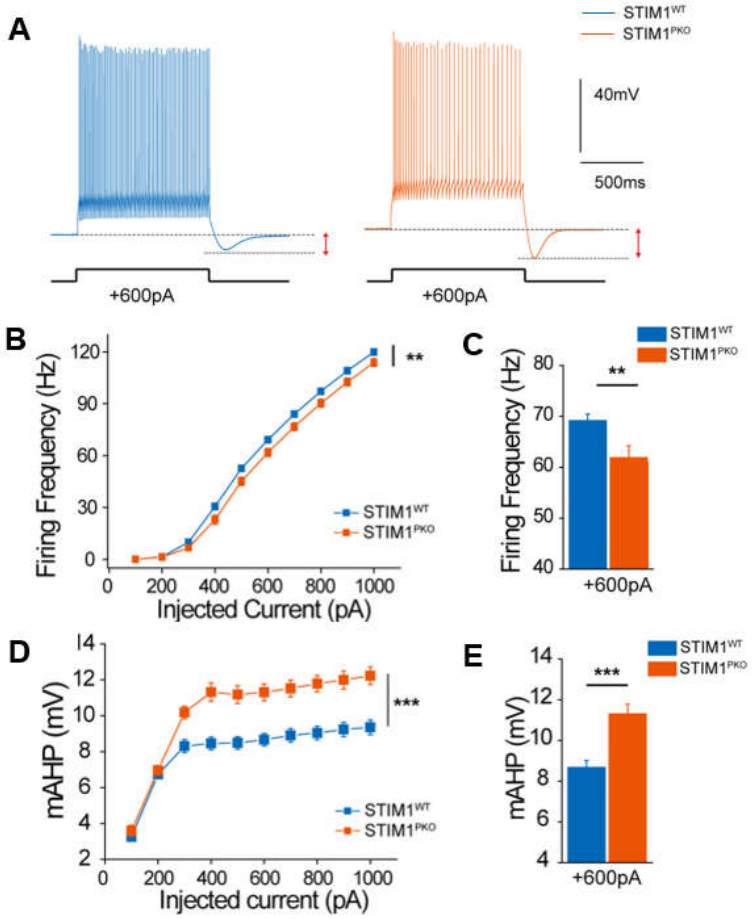

Figure 4. Current injection-evoked firing rate was decreased with increased mAHP in STIM1^{PKO}.

A, Representative trace at 600pA of current injection. **B**, Evoked firing rate was decreased in STIM1^{PKO} (STIM1^{WT}, n = 60; STIM1^{PKO}, n = 43). **C**. Bar graph at 600pA of current injection. **D**, The amplitude of mAHP significantly increased in STIM1^{PKO}. **E**, Bar graph at 600pA injection (right). Error bars denote SEM. **p<0.01, ***p<0.001.

Figure 5

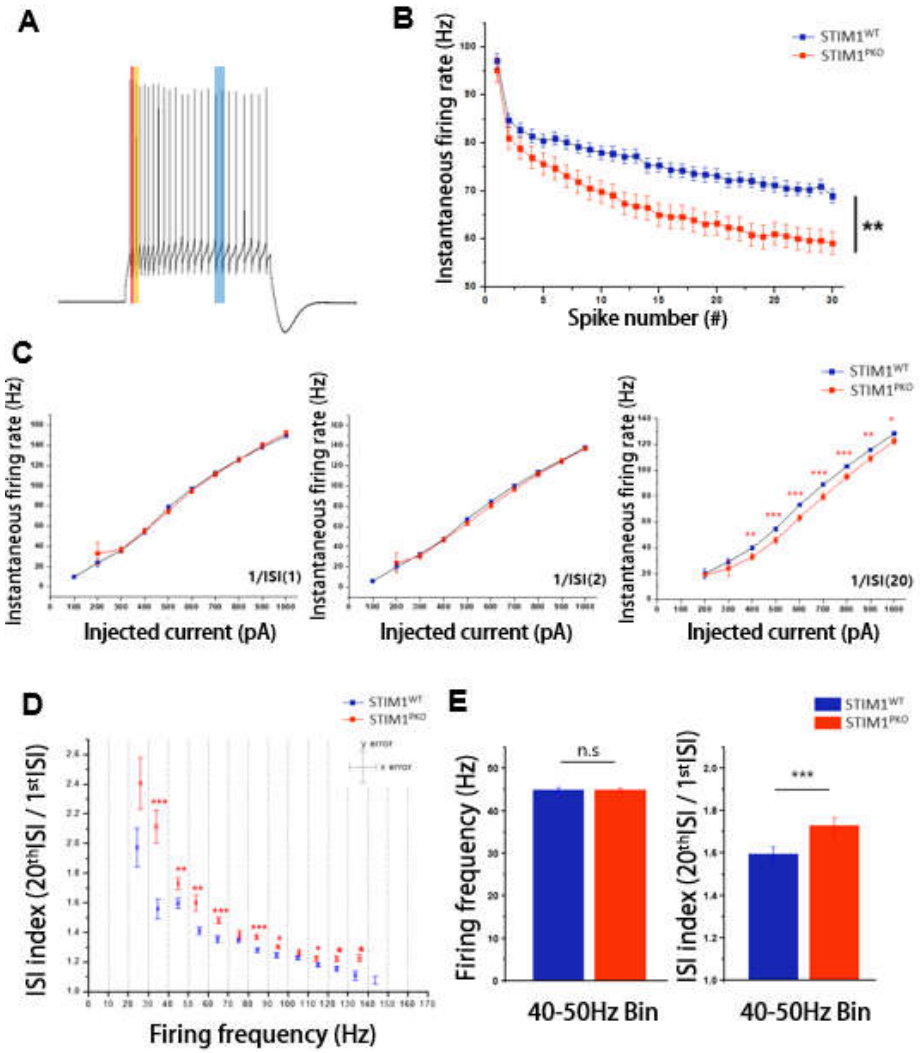
A
B
Instantaneous firing rate (Hz)
STIM1WT
STIM1PKO
**
Spike number (#)
C
Instantaneous firing rate (Hz)
1/ISI(1)
Injected current (pA)
1/ISI(2)
1/ISI(20)
D
ISI index (20thISI / 1stISI)
Firing frequency (Hz)
E
Firing frequency (Hz)
n.s
40-50Hz Bin
ISI index (20thISI / 1stISI)
***

Figure 5. SFA was strengthened in STIM1^{PKO}, which indicated different firing pattern.

A, Representative trace of current injection-evoked firing. Red, yellow and blue box indicate 1st, 2nd and 3rd spike of the spike train. **B**, Instantaneous firing frequency was more steeply decreased in STIM1^{PKO}, which signifies strengthened SFA (STIM1^{WT}, n = 60; STIM1^{PKO}, n = 43). **C**, Instantaneous firing rate for 1st (left), 2nd (middle) and 20th (right) ISI. Not initial but latter instantaneous firing showed remarkable differences at almost all injected current condition (Same data set of B). **D**, Graph showing ISI indices (20th ISI/1st ISI) to the bins of firing frequency (bin size: 10Hz). Data showed STIM1^{PKO} had distinctive difference in ISI index despite of the similar frequency (Same data set of B). **E**, Bar graph of firing frequencies (left) and ISI indices (right) of STIM1^{WT} and STIM1^{PKO} in 40-50Hz bin. Error bars denote SEM. *p<0.05, **p<0.01, ***p<0.001.

Figure 6

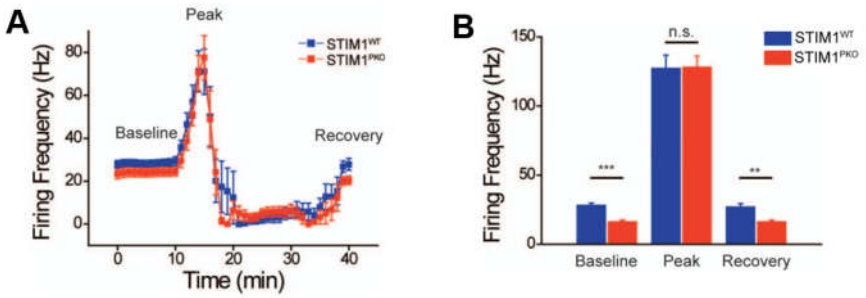

Figure 6. Low Ca^{2+} ACSF narrowed the difference in spontaneous firing rate between $STIM1^{WT}$ and $STIM1^{PKO}$.

A, Continuous cell-attached recording during the application of ACSF containing low Ca^{2+} concentration. Under low extracellular Ca^{2+} concentration (100μM), firing rates of both groups increased and reached a similar peak point within 5 min. When extracellular Ca^{2+} concentration returned to normal (2mM), the firing rate slowly recovered to the initial level ($STIM1^{WT}$, n = 15; $STIM1^{PKO}$, n = 14). **B**, Bar graph of low-Ca^{2+} contained ACSF application. Error bars denote the SEM. **p < 0.01, ***p < 0.001.

Figure 7

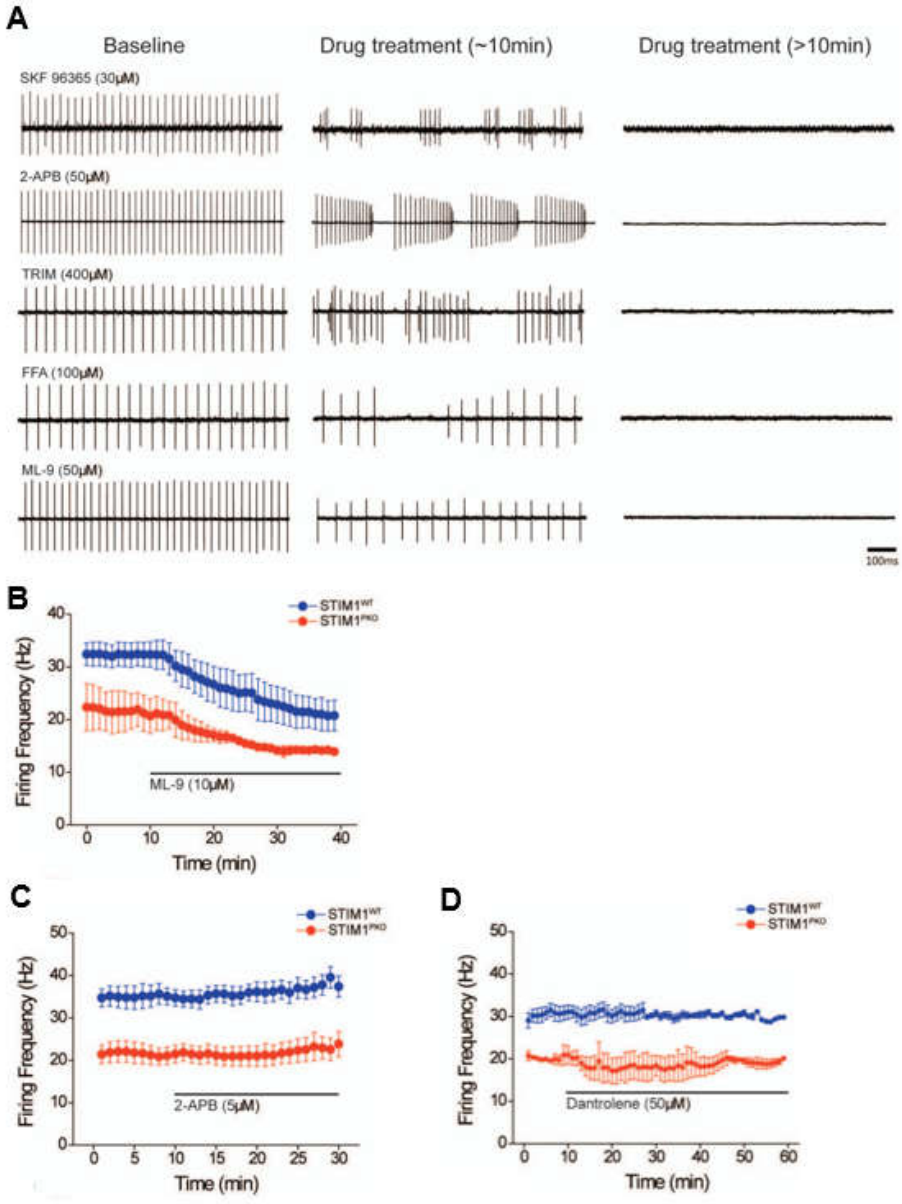
A
Baseline
Drug treatment (~10min)
Drug treatment (>10min)
SKF 96365 (30μM)
2-APB (50μM)
TRIM (400μM)
FFA (100μM)
ML-9 (50μM)
100ms
B
STIM1WT
STIM1PKO
Firing Frequency (Hz)
ML-9 (10μM)
Time (min)
C
STIM1WT
STIM1PKO
Firing Frequency (Hz)
2-APB (5μM)
Time (min)
D
STIM1WT
STIM1PKO
Firing Frequency (Hz)
Dantrolene (50μM)
Time (min)

Figure 7. Blocking SOCE or CICR could not reduce the difference of firing rate between $STIM^{WT}$ and $STIM^{PKO}$.

A, Various SOCE blockers changed firing pattern of Purkinje neuron and finally caused firing failure. Time points, from left to right, baseline, before firing failure with pattern changes (usually until 10min) and after firing failure (usually after 10min). Drugs, from top to bottom, SKF 96365 (30μM), non-specific SOCE blocker. High concentration of 2-APB (50μM), non-specific SOCE blocker. TRIM (400μM), non-specific SOCE blocker. FFA (100μM), TRPC3 and 7 blocker. ML-9 (50μM), STIM1-plasma membrane interaction blocker. **B**, Partial blocking of SOCE by ML-9 (10μM). Since ML-9 reduces firing rate without pattern change, we partially blocked to prevent firing failure. However, firing rates of both $STIM1^{WT}$ and $STIM1^{PKO}$ were equally reduced ($STIM1^{WT}$, n = 3; $STIM1^{PKO}$, n = 2). **C** and **D**, The firing rate of Purkinje neuron was not affected by blocking CICR. **C**, Lower concentraion of 2-APB (5μM) to block IP3 receptor ($STIM1^{WT}$, n = 5; $STIM1^{PKO}$, n = 5) and **D**, blocking ryanodine receptor by Dantrolene ($STIM1^{WT}$, n = 6; $STIM1^{PKO}$, n = 2) were not able to change firing rate of Purkinje neurons in both groups.

Figure 8

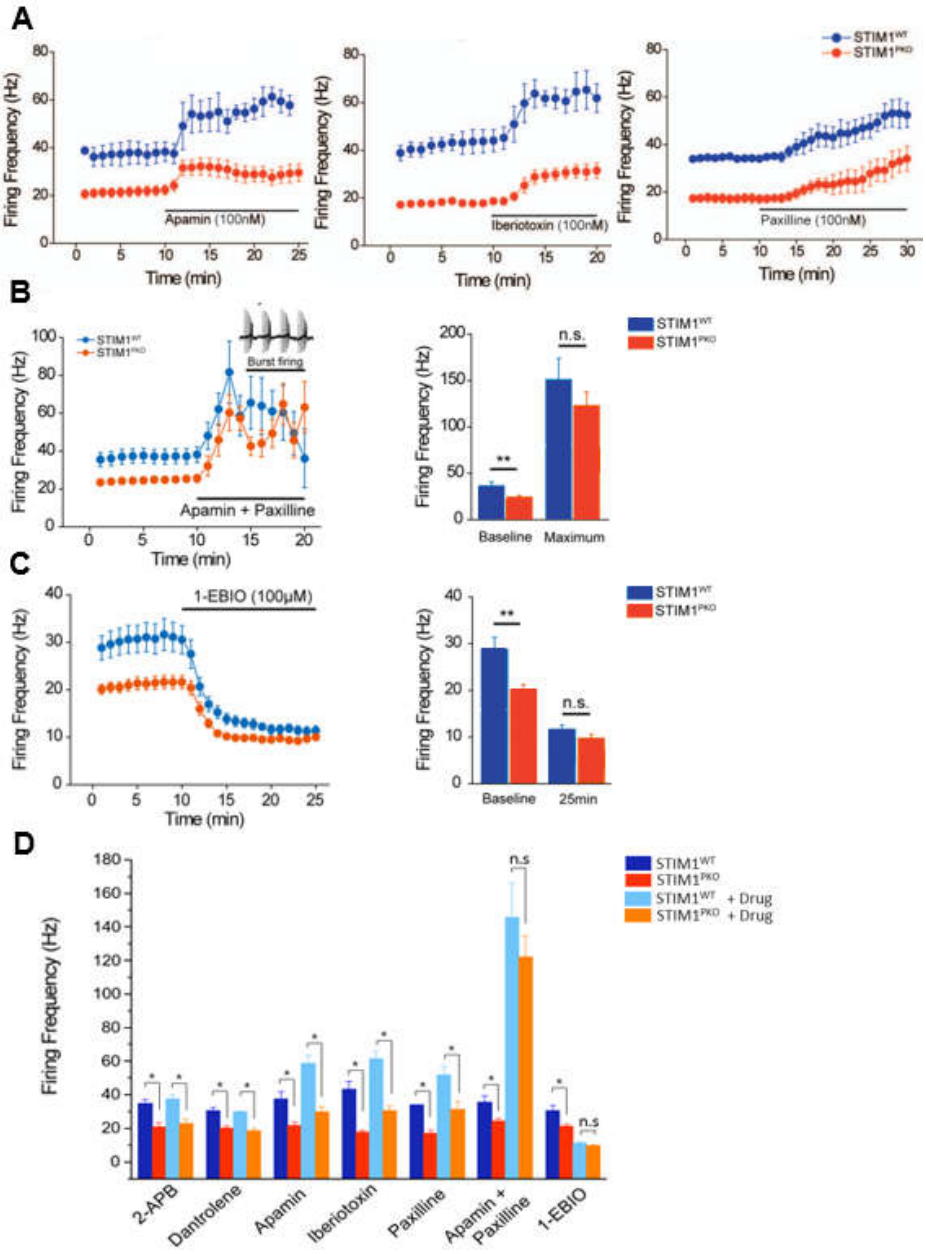
A
Firing Frequency (Hz)
Time (min)
Apamin (100nM)
Iberiotoxin (100nM)
Paxilline (100nM)
STIM1WT
STIM1PKO
B
Burst firing
Apamin + Paxilline
n.s.
**
Baseline
Maximum
C
1-EBIO (100μM)
25min
D
STIM1WT + Drug
STIM1PKO + Drug
2-APB
Dantrolene
Apamin
Iberiotoxin
Paxilline
Apamin + Paxilline
1-EBIO

Figure 8. Activation of Ca^{2+}-activated K^+ channels was required for altering excitability of $STIM1^{PKO}$.

A, Blocking SK channel (by apamin (100nM), left, $STIM1^{WT}$, n = 3; $STIM1^{PKO}$, n = 13) or BK channel (by iberiotoxin (100nM), middle, $STIM1^{WT}$, n = 3; $STIM1^{PKO}$, n = 4; by paxilline (100nM), a broader spectrum blocker that is able to block iberiotoxin-insensitive BK currents, right, $STIM1^{WT}$, n = 2; $STIM1^{PKO}$, n = 6) was not able to reduce the difference in firing rate between two groups. **B**, Blocking both SK and BK channels with the cocktail of apamin (100nM) and paxilline (100nM). The mixture of drugs narrowed the gap in firing rates between $STIM1^{WT}$ and $STIM1^{PKO}$ ($STIM1^{WT}$, n = 7; $STIM1^{PKO}$, n = 9). Although blocking both SK and BK channels suddenly changed the firing pattern (from tonic firing to burst firing), the firing frequencies of both groups became similar before pattern change (left). Bar graph in two time points (right). Baseline is before drug treatment, and maximum is the maximum firing rate before pattern change. In the comparison of maximum firing rates, there was no statistical significance between $STIM1^{WT}$ and $STIM1^{PKO}$. **C**, Potentiating Kca channels with 1-EBIO (100μM). 1-EBIO treatment decreased the difference between $STIM1^{WT}$ and $STIM1^{PKO}$ mice without changing the firing pattern (left; $STIM1^{WT}$, n = 7; $STIM1^{PKO}$, n = 15). The bar graph shows the baseline and 15min after drug application (right). At 15 min after 1-EBIO treatment, statistical significance between $STIM1^{WT}$ and $STIM1^{PKO}$ disappeared. Error bars denote the SEM. **D,** Bar graph summarizing the data from Figure 5C-D and Figure 6B-D. Error bars denote the SEM. *$p<0.05$, **$p < 0.01$.

Figure 9

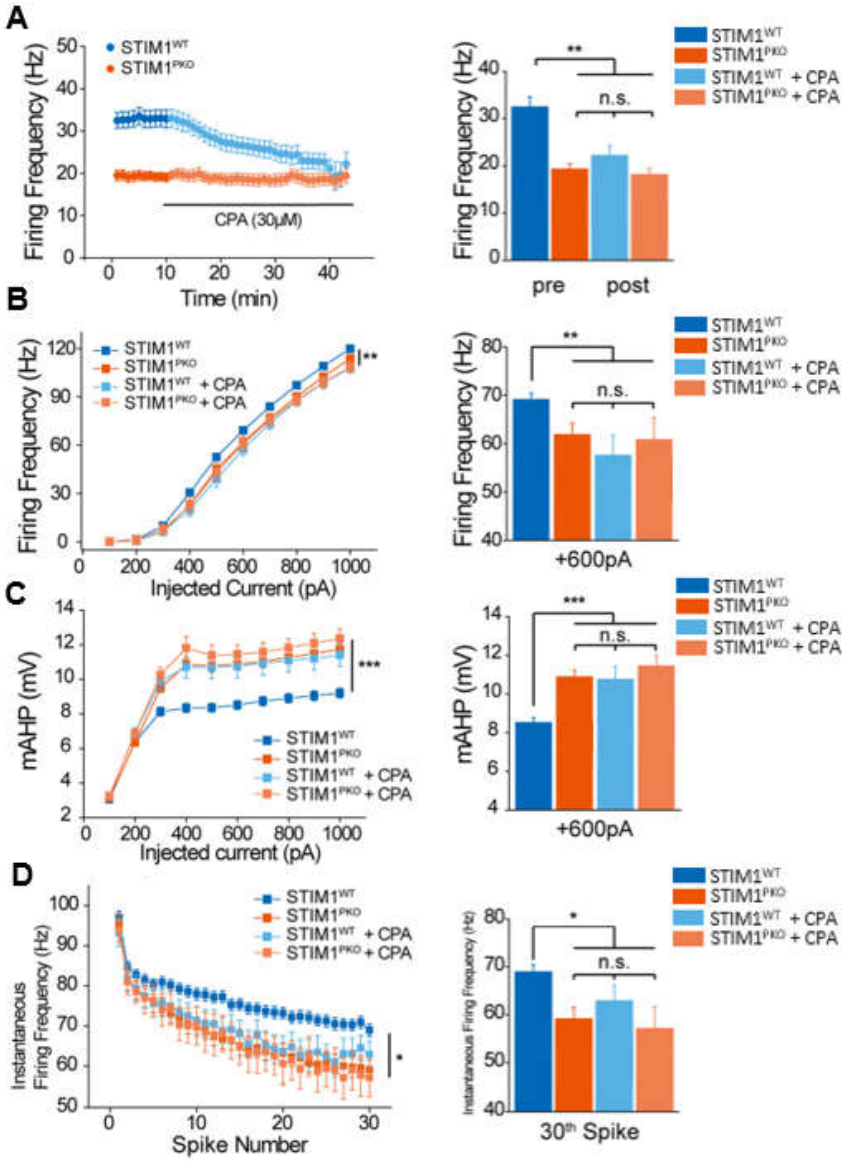
A
Firing Frequency (Hz)
STIM1WT
STIM1PKO
CPA (30μM)
Time (min)
B
Firing Frequency (Hz)
STIM1WT + CPA
STIM1PKO + CPA
Injected Current (pA)
C
mAHP (mV)
Injected current (pA)
D
Instantaneous Firing Frequency (Hz)
Spike Number
n.s.
pre
post
+600pA
30th Spike

Figure 9. Blocking SERCA reproduced the attenuated intrinsic excitability of STIM1^{PKO}.

A, CPA treatment during the attached recording. CPA (30μM) decreased firing rates of STIM1^{WT} to the level of STIM1^{PKO}, while STIM1^{PKO} seemed to be unaffected by CPA (STIM1^{WT}, n = 11; STIM1^{PKO}, n = 9). Comparing initial firing rates to 30 min after CPA treatment, the initial firing rates of STIM1^{WT} are remarkably higher than any others. **B**, 30 min of CPA (30μM) pre-incubation reduced the evoked firing rate of STIM1^{WT}.STIM1^{WT} showed significantly higher evoked firing frequency than other groups (STIM1^{WT}, n = 60; STIM1^{PKO}, n = 43; STIM1WT + CPA, n = 17; STIM1^{PKO} + CPA, n = 13). At the 600pA point, the differences between wild-type mice and others are obvious (right). **C**, mAHP after pre-incubation of CPA. Only the Purkinje neurons of STIM1^{WT} were affected by the drug, and mAHP of STIM1^{WT} became same as other groups. The representative bar graph at 600 pA of current injection shows that STIM1^{WT} had considerably smaller mAHP than other groups. **D**, CPA strengthened the SFA of STIM1^{WT}. The instantaneous firing frequency at the 30th spike was significantly lower in the other three groups than STIM1^{WT}. Data from drug-untreated STIM1^{WT} and STIM1^{PKO}, except A, were pooled from Figure 3. Error bars denote the SEM. *$p < 0.05$; **$p < 0.01$; ***$p < 0.001$.

Figure 10

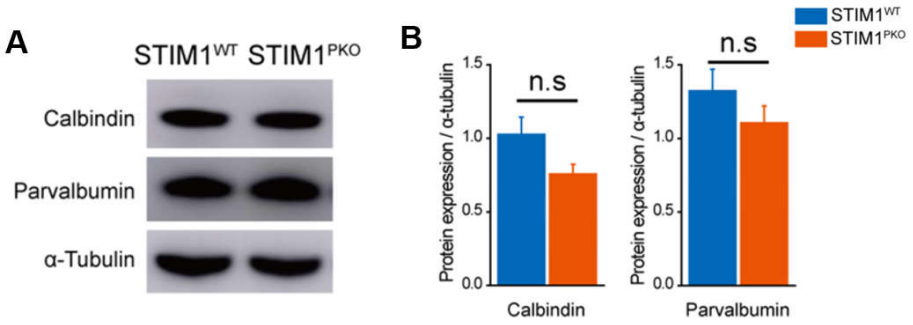

Figure 10. STIM1 deletion did not significantly change the expression level of Ca^{2+}-buffer proteins.

A, Representative Western blot bands for calbindin-D28k and parvalbumin. **B**, There was no significant difference in the abundance of calbindin-D28k and parvalbumin ($STIM1^{WT}$, n = 6; $STIM1^{PKO}$, n = 5). Each protein expression level was normalized by α-tubulin in the same lane.

Table 1

		$STIM1^{WT}$	$STIM1^{PKO}$	p-value
Cm (pF)		644.9 ± 12.7	634.5 ± 14.0	0.586
Rin (MΩ)		**43.9 ± 1.1**	**38.1 ± 1.0**	**< 0.001*** **
First spike latency (msec)		16.5 ± 0.5	18.0 ± 0.9	0.159
Rheobase (pA)		261.1 ± 9.1	281.6 ± 11.2	0.159
Threshold (mV)	1st spike	-47.0 ± 0.3	-46.0 ± 0.5	0.080
	25th spike	-43.1 ± 0.4	-41.9 ± 0.5	0.070
AP amplitude (mV)	1st spike	82.0 ± 1.0	82.4 ± 1.1	0.775
	25th spike	70.6 ± 1.0	71.4 ± 1.0	0.545
FWHM (msec)	**1st spike**	**0.205 ± 0.004**	**0.195 ± 0.003**	**0.031***
	25th spike	**0.226 ± 0.005**	**0.211 ± 0.003**	**0.012***
Upstroke ($V \cdot s^{-1}$)	1st spike	542.6 ± 10.1	570.1 ± 10.3	0.059
	25th spike	**421.0 ± 9.8**	**448.5 ± 8.8**	**0.039***
Downstroke ($V \cdot s^{-1}$)	1st spike	-452.9 ± 10.9	-466.0 ± 9.6	0.368
	25th spike	-368.8 ± 10.3	-385.9 ± 9.1	0.214
fAHP (mV)	1st spike	14.6 ± 0.3	14.3 ± 0.4	0.581
	25th spike	15.8 ± 0.3	15.9 ± 0.4	0.830
Slope of post-spike depolarization (V·s-1)	1st spike	1.69 ± 0.03	1.62 ± 0.05	0.234
	25th spike	**1.19 ± 0.03**	**1.01 ± 0.04**	**<0.001*** **
ISI (ms)	1st spike	10.4 ± 0.2	10.7 ± 0.3	0.402
	25th spike	**14.4 ± 0.3**	**17.3 ± 0.8**	**<0.001*** **
Postburst mAHP (mV)		**8.5 ± 0.3**	**10.9 ± 0.3**	**< 0.001*** **

Table 1. Passive and active membrane properties of $STIM1^{WT}$ and $STIM1^{PKO}$.

Several parameters, including Rin, slope of postspike depolarization, ISI, and mAHP were significantly different in $STIM1^{PKO}$ compared to $STIM1^{WT}$. Active properties of the 25th spike showed more differences than those of the 1st spike. Slope of post-spike depolarization, especially, were remarkably lowered in $STIM1^{PKO}$, which could explain the increase of ISI despite the shortened action potential waveform. Up-stroke and down-stroke, rising and falling phase of action potential, respectively. Data were from the experiment performed in Figure 3. Data are expressed as mean±SEM. *$p<0.05$, ***$p<0.001$.

Discussion

The role of ER store in firing neuron; STIM1, SERCA and Ca2+ clearance

For about recent 10 years, there have been intensive studies identifying the role of STIM1 in refilling ER store by inducing SOCE (Soboloff et al., 2012). Because of its importance on SOCE, STIM1 have been studied mostly in non-excitable cells, especially immune cells (lymphocytes and mast cells), where SOCE is the major pathway of intracellular Ca2+ influx (Liou et al., 2005; Roos et al., 2005). In neurons, however, Ca2+ influx mainly occur through voltage-gated ion channel (VGCC). Furthermore, Purkinje neurons have distinctive property; spontaneous firing activity so they seem to have Ca^{2+}-rich environment than any other neuron. These circumstances seem to make it hard to explain the reason of the highest expression of STIM1 in Purkinje neurons only with the canonical role of STIM1.

For normal physiological function, entered Ca^{2+} should be cleared properly to keep Ca^{2+} homeostasis. It has been reported that STIM1 can recruit partner of STIM1 (POST) proteins to interact PMCA and SERCA (Krapivinsky et al., 2011) which are known to extrude cytosolic Ca2+ into extracellular space and internal store, respectively. STIM1-POST complex, however, act in opposite way; it enhances SERCA while it inhibits PMCA (Ritchie et al., 2012; Jousset et al., 2007). In Purkinje neurons, as SERCA have much more influence on extruding cytosolic Ca^{2+} than PMCA (Fierro et al., 1998), the net effect of STIM1 would enhance SERCA function. Our data also correspond to these results in that altered intrinsic properties in $STIM1^{PKO}$ was due to hypofunction of SERCA. We demonstrated that STIM1 and SERCA have essential role on maintaining the regularity and the excitability of firing by clearing Ca^{2+} in Purkinje neurons where depolarization-induced Ca^{2+} influx continuously occurs. This concept of buffering Ca^{2+}

by SERCA is supported by several previous studies (Cueni et al., 2008; Higgins et al., 2006).

So far, the event of pumping cytosolic Ca2+ into ER store by SERCA has been focused as the aspects of refilling depleted ER. On the other hand, from the view of cytosol, same event can be interpreted into sequestration of Ca^{2+}, preventing accumulation. In this paper, we suggest the important point of view that ER in neurons is not only the object that should be refilled for releasing Ca^{2+} into cytosol, but also the sink for sequestrating cytosolic Ca^{2+} effectively.

Spike frequency adaptation and its underlying mechanism

SFA is a universal mechanism of the nervous system which self-reduces frequency to a constant input. Underlying mechanisms of SFA are mostly attributed to two kinds of ionic current, the voltage-gated M-type K+ current (M-current) and the calcium-activated K+ current (Kca current) (Benda et al., 2003; Prescott et al., 2008). M-current, which mediates subthreshold adaptation, is known to increase rheobase or threshold without changing *f-I* slope, whereas K_{Ca} current, which mediates spike-triggered adaptation, lowers *f-I* slope without alteration in rheobase or threshold (Deemyad et al., 2012). In our results, $STIM1^{PKO}$ showed lower *f-I* slope than $STIM1^{WT}$ with no difference in rheobase. Moreover, $STIM1^{PKO}$ had larger mAHP which is dependent on Kca current in various neurons including Purkinje neurons. Although our experimental results suggest that strengthened SFA and the consequent reduction in spontaneous firing rate was due to the change in Kca current, no single kind of Kca channels such as SK or BK could not explain the results. Instead, blocking or enhancing both SK and BK channels made spontaneous firing rate of $STIM1^{PKO}$ to reach the level of $STIM1^{WT}$.

Spatiotemporal arrangement of Ca^{2+}-dependent effectors around Ca^{2+} influx sources on plasma membrane, called "Ca^{2+} nano/micro domain", tightly regulates activities of K_{Ca} channels, and the domain is confined by various kinds of Ca^{2+} buffer and pump systems (Fakler and Adelman, 2008). In addition, a previous study identified the function of SERCA as a Ca^{2+} domain regulator in neurons (Cueni et al, 2008). We hypothesize that deletion of STIM1, making Ca^{2+} buffering and pumping activity of SERCA improper, could disrupt balanced Ca^{2+} nano/micro domain, thus changing activities of all K_{Ca} channels including both BK and SK channels.

Meanwhile, there are not only Kca or M- current but also other ionic currents that contribute to SFA such as a slow inactivation of persistent Na^{+} current (Fleidervish et al., 1996). Recent studies reported anontamin-2 (ANO2), one of Ca^{2+}-acitvated Cl^{-} channel (CACC), is widely expressed in brain region including cerebellum (Zhang et al., 2015) and mediates SFA in thalamocortical neurons (Ha et al., 2016). In addition, an alteration in SERCA activity is able to induce changes in Na^{+} (Louch et al., 2010), which make changes in Ca2+ dynamics and can contribute to SFA in other way. However, the precise mechanism explaining SERCA-dependent increase of SFA in $STIM1^{PKO}$ remains to be clarified.

A candidate for mediating the regulation of STIM1 to SERCA

This study shows the results that STIM1-assisted SERCA function is important for clearing cytosolic Ca2+ influx and regulating intrinsic excitability in firing neurons, which means STIM1 in Purkinje neurons might be constitutively activated in some degree as Purkinje neuron fires almost all the time. Previous studies reported that STIM1 can co-localize with SERCA2b (one of the main SERCA isotypes in Purkinje neuron)

at puncta (Manjarrés et al., 2010) and this is enabled by STIM1-POST complex which can bind to SERCA2 (Krapivinsky et al., 2011). However, they demonstrated that activation of POST requires depletion of ER Ca^{2+}. As our result showed (Figrue 2), ER stores in Purkinje neurons have less chance to be depleted because of Ca2+ influx from a number of VGCC. Therefore, in Purkinje neuron's circumstances, POST is not the strong candidate for mediator between STIM1 and SERCA. In other cell types, there have been a lot of studies about various molecules modulating SERCA. In heart, for instance, the role of phospholamban (PLB) is well established as a regulator of cardiac contractibility by binding and inhibiting SERCA2a (the main SERCA isotype in cardiac cell) depending on its phosphorylation state ((MacLennan and Kranias, 2003). Recent study reported that STIM1 can bind to and neutralize PLB, thus making dis-inhibiting effect in ventricular myocytes (Zhao et al., 2016) The important thing is STIM1 activation in ventricular myocyte was not dependent on SR Ca^{2+} store. However, PLB was expressed in neither cerebrum or cerebellum (Plessers et al., 1991) Instead, there are ER chaperones, calreticulin (CRT) and calnexin (CNX), which are expressed in brain and inhibit SERCA activity like PLB (Roderick et al., 2000). Moreover, CNX but not CRT was identified as a novel binding partner of STIM1 by using co-immunoprecipitation (Saitoh et al., 2011). In addition, both CNX and SERCA2b are also highly expressed in Purkinje neurons and widely distributed from cell body to dendritic spines (Villa et al., 1992; Sepulveda et al., 2004) so CNX might be the reasonable candidate for mediator of STIM1 and SERCA.

There has been a report that activation of PKC, by using PKC activator (0.5μM PDBu), accelerates AP-induced Ca^{2+} clearance in sensory neurons and this was mediated by PMCA and SERCA, competitively (Usachev et al., 2006). We tested the

effect of PKC in Purkinje neuron and observed that PDBu gradually increased spontaneous firing rate and that was occluded by CPA (data not shown). These results are rather ambiguous because PKC activation influence not only ER chaperone but also numerous factors that are also important for spontaneous firing although it was occluded by CPA.

Another candidate is ERp57, one of ER chaperones, that is also reported to have novel binding with STIM1 (Saitoh et al., 2012) ERp57 modulates SERCA by redox regulation (Li and Camacho, 2003). Mechanisms under association with chaperone proteins, there would be two plausible hypotheses. One is that the phosphorylation of chaperon proteins was affected as altered SOCE, assumably, exert local control of adenylyl cyclases (Lefkimmiatis et al., 2009). The other is that STIM1 binding to chaperon proteins make them neutralize and induce dis-inhibiting effect. The regulation mechanism of SERCA by STIM1 in Purkinje neuron requires further study and through this, we could take one step forward to the understanding of the principles on firing neuron's physiology.

References

Akita, T. and Kuba, K. (2000). Functional Triads Consisting of Ryanodine Receptors, Ca2+Channels, and Ca2+-Activated K+Channels in Bullfrog Sympathetic Neurons. The Journal of General Physiology, 116(5), pp.697-720.

Bastianelli, E. (2003). Distribution of calcium-binding proteins in the cerebellum. The Cerebellum, 2(4), pp.242-262.

Bean, B. (2007). The action potential in mammalian central neurons. Nature Reviews Neuroscience, 8(6), pp.451-465.

Belmeguenai A, Hosy E, Bengtsson F, Pedroarena C, Piochon C, Teuling E, He Q, Ohtuski G, De Jeu MT, Elgersma Y, De Zeeuw CI, Jorntell H, Hansel C (2010) Intrinsic plasticity complements long-term potentiation in parallel fiber input gain control in cerebellar Purkinje cells. J Neurosci 30:13630–13643

Benda J, Herz AVM (2003) A universal model for spike-frequency adaptation. Neural Comput 15:2523–2564

Benton MD, Lewis AH, Bant JS, Raman IM (2013) Iberiotoxin-sensitive and -insensitive BK currents in Purkinje neuron somata. J Neurophysiol 109:2528–2541

Brenowitz SD, Best AR, Regehr WG (2006) Sustained elevation of dendritic calcium evokes widespread endocannabinoid release and suppression of synapses onto cerebellar

Purkinje cells. J Neurosci 26:6841–6850

Cueni L, Canepari M, Luján R, Emmenegger Y, Watanabe M, Bond CT, Franken P, Adelman JP, Lüthi A (2008) T-type Ca2+ channels, SK2 channels and SERCAs gate sleep-related oscillations in thalamic dendrites. Nat Neurosci 11:683–692

Dean P, Porrill J, Ekerot C-F, Jörntell H (2010) The cerebellar microcircuit as an adaptive filter: experimental and computational evidence. Nat Rev Neurosci 11:30–43

Deemyad, T., Kroeger, J. and Chacron, M. (2012). Sub- and suprathreshold adaptation currents have opposite effects on frequency tuning. The Journal of Physiology, 590(19), pp.4839-4858.

Edgerton, J. and Reinhart, P. (2003). Distinct contributions of small and large conductance Ca2+-activated K+ channels to rat Purkinje neuron function. The Journal of Physiology, 548(1), pp.53-69.

Fakler, B. and Adelman, J. (2008). Control of KCa Channels by Calcium Nano/Microdomains. Neuron, 59(6), pp.873-881.

Fierro L, DiPolo R, Llano I (1998) Intracellular calcium clearance in Purkinje cell somata from rat cerebellar slices. J Physiol 510:499–512

Fleidervish, I., Friedman, A. and Gutnick, M. (1996). Slow inactivation of Na+ current

and slow cumulative spike adaptation in mouse and guinea-pig neocortical neurones in slices. The Journal of Physiology, 493(1), pp.83-97.

Ha, G., Lee, J., Kwak, H., Song, K., Kwon, J., Jung, S., Hong, J., Chang, G., Hwang, E., Shin, H., Lee, C. and Cheong, E. (2016). The Ca2+-activated chloride channel anoctamin-2 mediates spike-frequency adaptation and regulates sensory transmission in thalamocortical neurons. Nature Communications, 7, p.13791.

Hartmann J, Karl RM, Alexander RPD, Adelsberger H, Brill MS, Rühlmann C, Ansel A, Sakimura K, Baba Y, Kurosaki T, Misgeld T, Konnerth A (2014) STIM1 Controls Neuronal Ca2+ Signaling, mGluR1-Dependent Synaptic Transmission, and Cerebellar Motor Behavior. Neuron 82:635–644

Higgins ER, Cannell MB, Sneyd J (2006) A buffering SERCA pump in models of calcium dynamics. Biophys J 91:151–163

Hoebeek, F., Stahl, J., van Alphen, A., Schonewille, M., Luo, C., Rutteman, M., van den Maagdenberg, A., Molenaar, P., Goossens, H., Frens, M. and De Zeeuw, C. (2005). Increased Noise Level of Purkinje Cell Activities Minimizes Impact of Their Modulation during Sensorimotor Control. Neuron, 45(6), pp.953-965.

Jousset, H., Frieden, M. and Demaurex, N. (2007). STIM1 Knockdown Reveals That Store-operated Ca2+Channels Located Close to Sarco/Endoplasmic Ca2+ATPases (SERCA) Pumps Silently Refill the Endoplasmic Reticulum. Journal of Biological Chemistry, 282(15), pp.11456-11464.

Ju, Y., Liu, J., Lee, B., Lai, D., Woodcock, E., Lei, M., Cannell, M. and Allen, D. (2011). Distribution and Functional Role of Inositol 1,4,5-trisphosphate Receptors in Mouse Sinoatrial Node. Circulation Research, 109(8), pp.848-857.

Krapivinsky, G., Krapivinsky, L., Stotz, S., Manasian, Y. and Clapham, D. (2011). POST, partner of stromal interaction molecule 1 (STIM1), targets STIM1 to multiple transporters. Proceedings of the National Academy of Sciences, 108(48), pp.19234-19239.

Lefkimmiatis, K., Srikanthan, M., Maiellaro, I., Moyer, M., Curci, S. and Hofer, A. (2009). Store-operated cyclic AMP signalling mediated by STIM1. Nature Cell Biology, 11(4), pp.433-442.

Li, Y. and Camacho, P. (2003). Ca2+-dependent redox modulation of SERCA 2b by ERp57. The Journal of Cell Biology, 164(1), pp.35-46.

Liou, J., Kim, M., Do Heo, W., Jones, J., Myers, J., Ferrell, J. and Meyer, T. (2005). STIM Is a Ca2+ Sensor Essential for Ca2+-Store-Depletion-Triggered Ca2+ Influx. Current Biology, 15(13), pp.1235-1241.

Louch, W.E., Hougen, K., Mørk, H.K., Swift, F., Aronsen, J.M., Sjaastad, I., Reims, H.M., Roald, B., Andersson, K.B., Christensen, G., Sejersted, O.M., 2010. Sodium accumulation promotes diastolic dysfunction in end-stage heart failure following Serca2 knockout. J. Physiol. 588, 465–478. doi:10.1113/jphysiol.2009.183517

MacLennan, D. and Kranias, E. (2003). Calcium: Phospholamban: a crucial regulator of cardiac contractility. Nature Reviews Molecular Cell Biology, 4(7), pp.566-577.

Manjarrés, I., Rodríguez-García, A., Alonso, M. and García-Sancho, J. (2010). The sarco/endoplasmic reticulum Ca2+ ATPase (SERCA) is the third element in capacitative calcium entry. Cell Calcium, 47(5), pp.412-418.

Mattson, M., LaFerla, F., Chan, S., Leissring, M., Shepel, P. and Geiger, J. (2000). Calcium signaling in the ER: its role in neuronal plasticity and neurodegenerative disorders. Trends in Neurosciences, 23(5), pp.222-229.

Neher, E. and Sakaba, T. (2008). Multiple Roles of Calcium Ions in the Regulation of Neurotransmitter Release. Neuron, 59(6), pp.861-872.

Plessers L, Eggermont JA, Wuytack F, Casteels R. (1991). A study of the organellar Ca2(+)-transport ATPase isozymes in pig cerebellar Purkinje neurons. J Neurosci, 11(3), 650-6.

Prescott, S. and Sejnowski, T. (2008). Spike-Rate Coding and Spike-Time Coding Are Affected Oppositely by Different Adaptation Mechanisms. Journal of Neuroscience, 28(50), pp.13649-13661.

Ritchie, M., Samakai, E. and Soboloff, J. (2012). STIM1 is required for attenuation of

PMCA-mediated Ca2+clearance during T-cell activation. The EMBO Journal, 31(5), pp.1123-1133.

Roderick, H., Lechleiter, J. and Camacho, P. (2000). Cytosolic Phosphorylation of Calnexin Controls Intracellular Ca2+Oscillations via an Interaction with Serca2b. The Journal of Cell Biology, 149(6), pp.1235-1248.

Roos, J., DiGregorio, P., Yeromin, A., Ohlsen, K., Lioudyno, M., Zhang, S., Safrina, O., Kozak, J., Wagner, S., Cahalan, M., Veliçelebi, G. and Stauderman, K. (2005). STIM1, an essential and conserved component of store-operated Ca2+channel function. The Journal of Cell Biology, 169(3), pp.435-445.

Saitoh, N., Oritani, K., Saito, K., Yokota, T., Ichii, M., Sudo, T., Fujita, N., Nakajima, K., Okada, M. and Kanakura, Y. (2011). Identification of functional domains and novel binding partners of STIM proteins. Journal of Cellular Biochemistry, 112(1), pp.147-156.

Sepulveda, M., Hidalgo-Sanchez, M. and Mata, A. (2004). Localization of endoplasmic reticulum and plasma membrane Ca2+-ATPases in subcellular fractions and sections of pig cerebellum. European Journal of Neuroscience, 19(3), pp.542-551.

Skibinska-Kijek A, Wisniewska MB, Gruszczynska-Biegala J, Methner A, Kuznicki J (2009) Immunolocalization of STIM1 in the mouse brain. Acta Neurobiol Exp 69:413–428

Soboloff, J., Rothberg, B., Madesh, M. and Gill, D. (2012). STIM proteins: dynamic calcium signal transducers. Nature Reviews Molecular Cell Biology, 13(9), pp.549-565.

Stiber, J., Hawkins, A., Zhang, Z., Wang, S., Burch, J., Graham, V., Ward, C., Seth, M., Finch, E., Malouf, N., Williams, R., Eu, J. and Rosenberg, P. (2008). STIM1 signalling controls store-operated calcium entry required for development and contractile function in skeletal muscle. Nature Cell Biology, 10(6), pp.688-697.

Sun S, Zhang H, Liu J, Popugaeva E, Xu N-JJ, Feske S, White CL, Bezprozvanny I (2014) Reduced synaptic STIM2 expression and impaired store-operated calcium entry cause destabilization of mature spines in mutant presenilin mice. Neuron 82:79–93

Terasaki, M., Slater, N., Fein, A., Schmidek, A. and Reese, T. (1994). Continuous network of endoplasmic reticulum in cerebellar Purkinje neurons. Proceedings of the National Academy of Sciences, 91(16), pp.7510-7514.

Usachev, Y., Marsh, A., Johanns, T., Lemke, M. and Thayer, S. (2006). Activation of Protein Kinase C in Sensory Neurons Accelerates Ca2+ Uptake into the Endoplasmic Reticulum. Journal of Neuroscience, 26(1), pp.311-318.

Verkhratsky A. (2005) Physiology and pathophysiology of the calcium store in the endoplasmic reticulum of neurons. Physiol Rev 85:201–279

Villa, A., Sharp, A., Racchetti, G., Podini, P., Bole, D., Dunn, W., Pozzan, T., Snyder, S. and Meldolesi, J. (1992). The endoplasmic reticulum of purkinje neuron body and

dendrites: Molecular identity and specializations for Ca2+ transport. Neuroscience, 49(2), pp.467-477.

Wulff, P., Schonewille, M., Renzi, M., Viltono, L., Sassoè-Pognetto, M., Badura, A., Gao, Z., Hoebeek, F., van Dorp, S., Wisden, W., Farrant, M. and De Zeeuw, C. (2009). Synaptic inhibition of Purkinje cells mediates consolidation of vestibulo-cerebellar motor learning. Nature Neuroscience, 12(8), pp.1042-1049.

Yamada, S., Takechi, H., Kanchiku, I., Kita, T. and Kato, N. (2004). Small-Conductance Ca2+-Dependent K+ Channels Are the Target of Spike-Induced Ca2+ Release in a Feedback Regulation of Pyramidal Cell Excitability. Journal of Neurophysiology, 91(5), pp.2322-2329.

Zhang, S., Yu, Y., Roos, J., Kozak, J., Deerinck, T., Ellisman, M., Stauderman, K. and Cahalan, M. (2005). STIM1 is a Ca2+ sensor that activates CRAC channels and migrates from the Ca2+ store to the plasma membrane. Nature, 437(7060), pp.902-905.

Zhang, W., Schmelzeisen, S., Parthier, D., Frings, S. and Möhrlen, F. (2015). Anoctamin Calcium-Activated Chloride Channels May Modulate Inhibitory Transmission in the Cerebellar Cortex. PLOS ONE, 10(11), p.e0142160.

Zhao, G., Zhang, H., Li, T., Brochet, D., Rosenberg, P. and Lederer, W. (2016). The Function of Stromal Interaction Molecule 1 (STIM1) in Heart. Biophysical Journal, 110(3), p.360a.

Zhou, H., Lin, Z., Voges, K., Ju, C., Gao, Z., Bosman, L., Ruigrok, T., Hoebeek, F., De Zeeuw, C. and Schonewille, M. (2014). Cerebellar modules operate at different frequencies. eLife, 3.

Abstract in Korean

신경세포의 기능에 있어서 세포질 내 칼슘의 적절한 조절은 매우 중요하다. 소포체는 상황에 따라 적절하게 세포질 내 칼슘이 드나들 수 있는 주된 세포 내 칼슘 저장소이다. 최근의 연구들은 STIM1이라고 하는 단백질이 이러한 소포체의 칼슘을 조절하는 기능을 담당하며 이 단백질은 뇌 전체, 특히 소뇌의 퍼킨지 신경세포에 높게 발현한다는 것을 밝혔다. 최근의 한 논문은 처음으로 퍼킨지 신경세포 내에서의 STIM1의 역할을 밝혔으며, 이는 대사성 글루타메이트 수용체 (mGluR1)을 통한 느린 전류의 매개체로서의 역할임을 보여준 것이었다. 그러나 이 실험들은 퍼킨지 신경세포와 같은 자발적 발화성 신경세포에서의 STIM1의 역할은 충분히 설명해주지 못하고 있다. 이에 우리는 퍼킨지 신경세포에 특이적으로 STIM1 유전자를 제거한 쥐를 사용하여 퍼킨지 신경세포에서의 STIM1의 기능적 역할을 조사하였다. 우리는 STIM1의 소실이 신호 자가 억제를 증대시키고 내인 흥분성을 축소시키는 결과를 얻었으며, 이는 칼슘 의존적 칼륨 채널 전류에 의한 것임을 밝혔다. 더 나아가 소포체칼슘펌프를 막는 것은 STIM1을 가진 야생형의 내인 흥분성을 STIM1이 없는 돌연변이형의 내인 흥분성 수준으로 떨어뜨리는 효과를 보였으며, STIM1이 없는 돌연변이형은 소포체칼슘펌프를 막는 것에 큰 영향을 받지 않았다. 이러한 결과들을 바탕으로, 이 논문은 퍼킨지 신경세포 내에서 STIM1의 주요 역할은 소포체칼슘펌프와 함께 세포질 내 칼슘을 처리함으로써 적절한 신경세포의 발화를 조절하는 것임을 제시하고 있다.

주요어 : 퍼킨지 신경세포, 자발적 발화성 신경세포, 내인 흥분성, STIM1, 소포체 칼슘 저장고, 소포체칼슘펌프

학 번 : 2013-21789